Robust speed control of brushless direct-drive motor using integral variable structure control

S.K.Chung
J.H.Lee
J.S.Ko
Prof. M.J.Youn

Indexing terms: Direct drive motor, Integral compensation, Load torque observer, Variable structure control

Abstract: A robust speed control technique for a brushless direct-drive motor (BLDDM) using a variable structure control (VSC) approach is presented. The significant problems of conventional VSC are investigated in view of the practical implementation and an integral variable structure control with a load torque observer is proposed as an effective way of overcoming these problems. By employing the proposed control scheme, the robustness against the unknown disturbance can be improved in the transient state and the steady-state error can be minimised by an integral action. Furthermore, the reduction of the chattering is also realised by using a load torque observer. The proposed algorithms are implemented using the software of DSP TMS320C30 and the effectiveness is verified through the comparative simulations and experiments for the BLDDM driven by a three phase voltage-fed PWM inverter.

List of symbols

r_s = stator resistance
L_q, L_d = q- and d-axis inductances, respectively
J = inertia moment of rotor and load
B = viscous friction coefficient
P = number of poles
i_q, i_d = q- and d-axis currents, respectively
V_q, V_d = q- and d-axis voltages, respectively
T_e = electromagnetic torque
T_L = load torque
p = Laplace operator
λ_m = linkage flux of permanent magnet
ω_r = electrical angular speed of the rotor
'^' = estimated value
'*ref*' = reference value
'*o*' = nominal value
'0' = initial value
'*min*' = minimum bound
'*max*' = maximum bound

IEE Proceedings online no. 19952230

Paper first received 29th November 1994 and in revised form 24th July 1995

S. K. Chung and Prof. M. J. Youn are with the Department of Electrical Engineering, Korea Advanced Institute of Science and Technology, 373-1, Kusong-Dong, Yusong-Gu, Taejon, 305-701, Korea

J. H. Lee is with the Department of Control & Instrumentation Engineering, Gyeongsang National University, 900, Gazwa-Dong, Jinju, Kyungsangnam-Do, 660-701, Korea

J. S. Ko is with the Production Engineering Center, Samsung Electronics Co., Ltd., 416, Maetan-3Dong, Paldal-Gu, Suwon, Kyungki-Do, 442-742, Korea

1 Introduction

Recently, brushless direct-drive motors (BLDDMs) without reduction gears are widely used in the high-performance servo applications such as industrial robots and machine tools. Since the BLDDM drive system does not require the reduction gear, a simple and reliable system can be achieved without any problems. It is, however, well known that the control performance of the BLDDM is very sensitive to load disturbance because the motor shaft is directly coupled with the external load. Thus, the speed control system of the BLDDM requires a more robust control technique against the load disturbance than that of conventional AC or DC motors with reduction gears. Various attempts to satisfy this requirement have been presented in the literature [1–6]. Among them, one of the attractive approaches is a variable structure control (VSC) technique which inherently has a robustness in the presence of the bounded uncertainty [7]. However, the VSC technique still has the some problems such as the reaching problem, chattering problem, and steady-state error because the ideal sliding mode cannot be achieved in practical applications [5–13].

The motion of the control system employing VSC can be described as two modes: reaching and sliding modes. The reaching mode means the control mode before the states of the system reach the predefined sliding surface in which the robustness of the VSC technique is not guaranteed. Thus, the predefined control characteristics cannot be achieved. For the design of the speed control system, the BLDDM is often modelled as a first-order system neglecting the electrical dynamics. Conventional VSC is not suitable for the first-order system because the whole transient state belongs to the reaching mode and the robustness against the unknown disturbance is not guaranteed in the whole transient state [13]. Because of this, most applications of VSC for the control of electric motors have been limited to the position servo system having

second-order dynamics [5, 6, 9–12]. To overcome this problem, the acceleration of the motor is introduced in the previous works [7, 8]. It is, however, difficult to obtain the information on the acceleration since the acceleration signal has generally high bandwidth and is very noisy.

Chattering is an inherent feature of VSC and causes the problems of producing vibration and wearing the mechanical parts of the actuator. In particular, it is highly undesirable for the speed control system of the BLDDM because the BLDDM is generally operated at low speed and under light load. Therefore the reduction technique of chattering should be considered for designing the speed control system of the BLDDM using VSC.

Theoretically, VSC is based on the assumption of the infinite switching action on the sliding surface. It is, however, difficult to meet this assumption in practice because of the limitations of the sampling frequency and control input. Thus, the ideal sliding motion having infinite switching action cannot be realised and this nonideal sliding motion is a factor of producing the undesirable steady-state error. Since the BLDDM drive system is usually implemented by using the digital control system with finite sampling frequency, and the control input is naturally limited by the ratings of the BLDDM and power device, the improving technique of steady-state performance should also be considered in the practical implementation of VSC.

In this paper, an integral variable structure control (IVSC) with a load-torque observer is proposed as an effective technique for overcoming the problems mentioned. Unlike conventional VSC, the IVSC is suitable for the first-order system without any information on the acceleration. Furthermore, the IVSC scheme provides not only a complete robustness without the reaching problem but also a good steady-state performance by the integral action. The reduction of chattering is also attempted by introducing the load torque observer. By a disturbance compensation technique using the load torque observer, the switching control of IVSC can be chosen as much smaller than that of the conventional scheme without disturbance compensation. As a result, chattering can be effectively reduced. The proposed control scheme is applied to the DSP-based BLDDM drive system and the effectiveness is well demonstrated through comparative simulations and experiments.

2 Modelling of brushless direct-drive motor

The BLDDM considered is a three-phase permanent magnet synchronous motor with sinusoidal back EMF. The stator windings are identical, displaced by 120°, and sinusoidally distributed. The nonlinear state equations of the BLDDM in the synchronous rotating reference frame can be expressed as follows [14]:

$$\frac{di_q}{dt} = -\frac{r_s}{L_q}i_q - \frac{L_d}{L_q}\omega_r i_d + \frac{1}{L_q}V_q - \frac{\lambda_m}{L_q}\omega_r \quad (1a)$$

$$\frac{di_d}{dt} = \frac{L_q}{L_d}\omega_r i_q - \frac{r_s}{L_d}i_d + \frac{1}{L_d}V_d \quad (1b)$$

$$T_e = \frac{3}{2}\left(\frac{P}{2}\right)[\lambda_m i_q + (L_d - L_q)i_q i_d] \quad (1c)$$

$$= J\left(\frac{2}{P}\right)\frac{d\omega_r}{dt} + B\left(\frac{2}{P}\right)\omega_r + T_L \quad (1d)$$

By employing the field-oriented control and stator current control, it can be assumed that the d-axis current i_d is controlled to be zero. Then, the electromagnetic torque in eqn. 1c can be linearised as

$$T_e = k_t i_q \quad (2)$$

where

$$k_t = \frac{3}{2}\left(\frac{P}{2}\right)\lambda_m$$

From eqns. 1 and 2 the mathematical model of the BLDDM can be simply described as

$$\frac{d\omega_r}{dt} = a_o\omega_r + b_o u + d_o f \quad (3)$$

where

$$u = i_q, \quad a_o = -\frac{B_o}{J_o}, \quad b = \frac{P}{2J_o}k_t, \quad d = -\frac{P}{2J_o}$$

and f is the unknown disturbance which includes the load torque and the effective torque caused by the changes of the inertia and viscous friction, and is defined as

$$f = T_L + \Delta J\left(\frac{2}{P}\right)\frac{d\omega_r}{dt} + \Delta B\left(\frac{2}{P}\right)\omega_r \quad (4)$$

where $\Delta J = J - J_o$, and $\Delta B = B - B_o$. In eqns. 1, 3 and 4, it is assumed that the parameters and load torque are bounded as

$$J_{min} < J_o + \Delta J < J_{max}$$

$$B_{min} < B_o + \Delta B < B_{max}$$

$$T_{Lmin} < T_L < T_{Lmax}$$

Fig. 1 shows a simplified block diagram of the speed control system for the BLDDM. If the state variable is chosen as $x = \omega_r - \omega_{ref}$ under the assumption that the speed reference ω_{ref} is constant, the resultant error state equation is derived as

$$\frac{dx}{dt} = a_o x + b_o u + a_o\omega_{ref} + d_o f \quad (5)$$

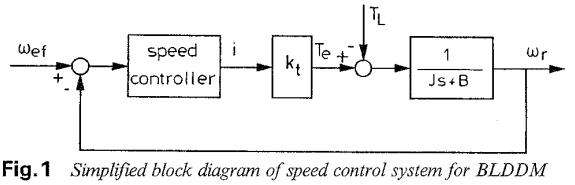

Fig. 1 *Simplified block diagram of speed control system for BLDDM*

3 Control strategy

3.1 IVSC for the first-order system

As can be seen in eqn. 5, the BLDDM is modelled as a first-order system. The conventional sliding surface for this system can be chosen as [7]

$$s = c_1 x = 0 \quad (6)$$

The expected time response of the state x is described as shown in Fig. 2. It is shown in this Figure that the sliding mode occurs only at the origin and the closed-loop system is operated like a high-gain linear feedback control system before the state x reaches the origin. In other words, the inherent switching action to reject the effect of the disturbance is not incurred in this region. It implies that the transient response of the system cannot be predefined by the dynamics of the sliding surface and the robustness which is a major advantage of

the VSC is not guaranteed in the whole transient state. It can be said, therefore that the direct application of the conventional VSC is not adequate in the first-order system.

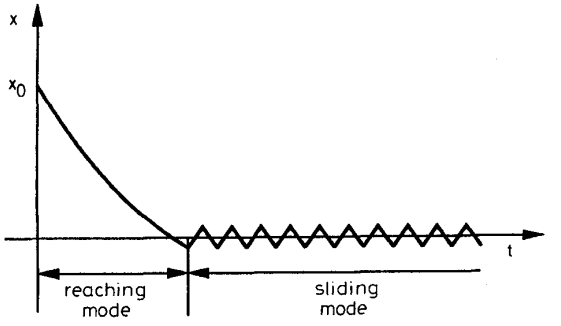

Fig.2 *Time responses of state x in first-order system: Conventional VSC*

To deal with this problem the sliding surface of the proposed control scheme is combined with the integration of the state x and is given as

$$s = x + c_1 \int_{-\infty}^{t} x(\tau)\, d\tau = 0 \tag{7}$$

The system dynamic equation can be expressed as

$$\dot{x} = -c_1 x \tag{8}$$

in the sliding mode. In eqn. 8, the state x exponentially approaches to zero with the time constant of $1/c_1$. The expected time response of the state x in the proposed IVSC is shown in Fig. 3. Note that the dynamic characteristics of the system can be predefined by choosing the coefficient c_1.

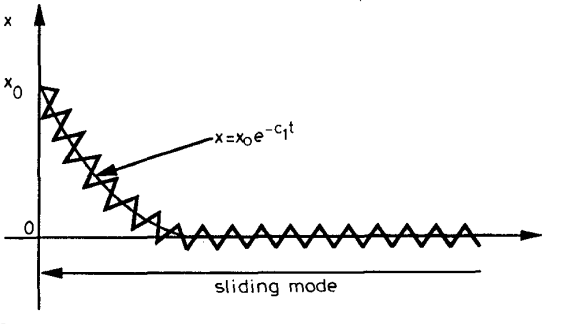

Fig.3 *Time responses of state x in first-order system: IVSC*

3.2 Complete robustness

Although introducing the IVSC gives predefined control characteristics in the transient state, it cannot be said that the sliding mode is guaranteed in the whole transient state. The system employing the IVSC has different dynamic responses depending on the initial condition of the integrator in the sliding surface. Only when the initial condition of the integrator is properly chosen, can the complete robustness be obtained in the whole transient state. At $t = 0$, eqn. 7 can be expressed as

$$x_0 + c_1 I_0 = 0 \tag{9}$$

where x_0 is the initial condition of the state x and I_0 is the initial condition of the integrator defined as

$$I_0 = \int_{-\infty}^{0} x(\tau)\, d\tau \tag{10}$$

From eqn. 9, I_0 to achieve the sliding mode at $t = 0$ can be derived as

$$I_0 = -\frac{x_0}{c_1} \tag{11}$$

If the initial condition of the integrator defined in eqn. 7 satisfies the condition given in eqn. 11, the sliding mode is always kept during entire response. Figs. 4 and 5 describe two different phase plane trajectories for the system with the IVSC. These Figures show that the sliding mode is ensured from the beginning of the response when the condition given in eqn. 11 is satisfied. In practice, since the initial condition of the state x is generally known, complete robustness can be realised by introducing the IVSC.

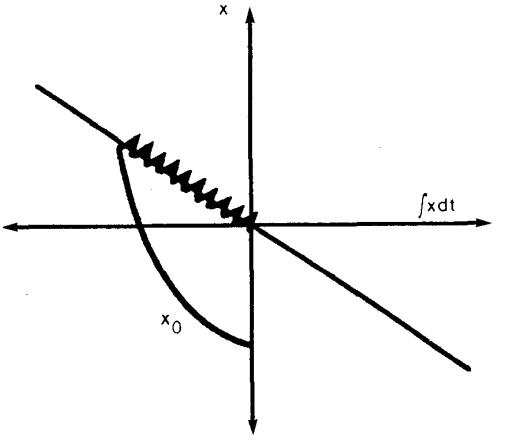

Fig.4 *Phase-plane trajectories of IVSC for initial condition of integrator:* $I_0 = 0$

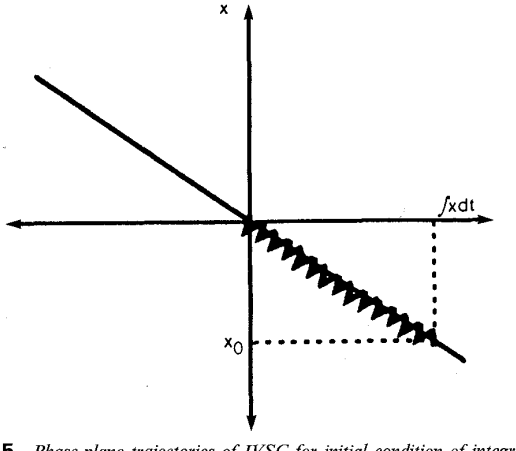

Fig.5 *Phase-plane trajectories of IVSC for initial condition of integrator:* $I_0 = -x_0/c_1$

The proposed IVSC scheme gives the additional advantage of improving the steady state performance [5, 12]. There exists the undesirable steady-state error owing to the nonideal sliding mode in the conventional VSC. However, the steady-state error can be effectively minimised by an integral action in the proposed IVSC scheme.

3.3 Chattering reduction using load torque observer

Since the BLDDM is generally operated at low speed region and under light load, the speed control perform-

ance is largely influenced by input chattering, i.e. the torque fluctuation. Thus, the reduction technique of the chattering is essential for the speed control of the BLDDM.

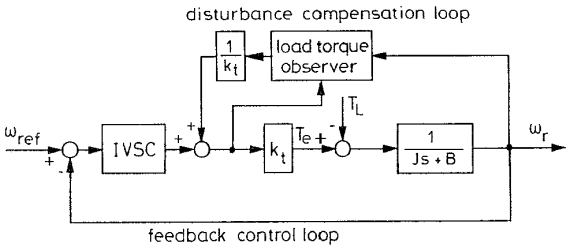

Fig. 6 *Control structure of proposed control scheme*

An interesting approach to reduce chattering is a disturbance compensation technique using a load torque observer [5, 6]. The basic idea of this approach is that the large portions of the unknown disturbance are compensated by the estimated disturbance of the load torque observer, and then the remaining portions are rejected by the IVSC employed as a feedback controller. Thus, the gains of the switching input in the IVSC can be chosen as much smaller than that of the IVSC without the disturbance compensation loop. Fig. 6 shows the overall structure of the proposed control scheme which consists of the IVSC and load torque observer.

4 Design of IVSC for speed control of BLDDM

The design procedure of the IVSC can be composed of the design of the sliding surface and the choice of the control input [7].

4.1 Design of sliding surface

The sliding surface of the proposed scheme is chosen as eqn. 7. The design parameters for this surface are the sliding surface coefficient c_1 and the initial condition of the integrator I_0. From eqn. 7, c_1 is chosen as a positive constant to satisfy the exponential stability and I_0 can be determined to satisfy the condition given in eqn. 11.

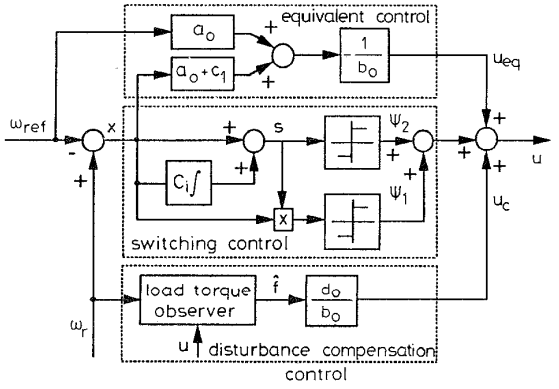

Fig. 7 *Control input structure of proposed control scheme*

4.2 Choice of control input

The control input of the proposed control scheme is composed of three different elements. It can be expressed as

$$u = u_{eq} + u_c + \Delta u \tag{12}$$

where u_{eq} equivalent control, u_c is the disturbance compensation term using the load torque observer, and Δu is the switching control. The input structure of the proposed scheme is described as shown in Fig. 7.

The equivalent control physically means the average value of the switching control in the sliding mode and is the same as the control for the exactly known parts of the BLDDM system. By using this control, the switching control Δu can be designed only for the unknown parts of the system and therefore the level of the switching control can be reduced [10]. From the equivalent control conditions given as $s = 0$ and $f = 0$ [7], u_{eq} is derived as follows:

$$u_{eq} = -\frac{1}{b_o}[(a_o + c_1)x + a_o\omega_{ref}] \tag{13}$$

The disturbance compensation term u_c can be obtained from the estimated disturbance of the load torque observer. If the estimated disturbance is $\hat{f}$, then u_c can be derived from eqn. 5 as

$$u_c = -\frac{d_o}{b_o}\hat{f} \tag{14}$$

After this compensation, the unknown parts of the system can be reduced as

$$\Delta f = f - \hat{f} \tag{15}$$

Thus, the switching control of the proposed control scheme can be chosen as much smaller than that of the conventional scheme without disturbance compensation. Therefore the reduction of chattering can be achieved by using this compensation technique.

The switching control Δu can be designed as

$$\Delta u = \Psi_1 x + \Psi_2 \tag{16}$$

where Ψ_1 and Ψ_2 are the switching functions. These are obtained from the sliding mode existence condition given as follows:

$$\begin{aligned}\frac{1}{2}\frac{d}{dt}(s^2) &= s\dot{s} \\ &= s[a_o x + b_o u + a_o\omega_{ref} + d_o f + c_1 x] \\ &= s[b_o\Psi_1 x + d_o\Delta f + b_o\Psi_2] \\ &< 0\end{aligned} \tag{17}$$

From the inequality in eqn. 17, Ψ_1 and Ψ_2 are given as follows:

$$\Psi_1 = \begin{cases} \alpha_1 > 0: & \text{if } sx < 0 \\ \beta_1 < 0: & \text{if } sx > 0 \end{cases} \tag{18a}$$

$$\Psi_2 = \begin{cases} \alpha_2 > -\dfrac{d_o}{b_o}\Delta f_{max}: & \text{if } s < 0 \\ \beta_2 < -\dfrac{d_o}{b_o}\Delta f_{min}: & \text{if } s > 0 \end{cases} \tag{18b}$$

4.3 Design of load torque observer for compensation of unknown disturbance

The unknown disturbance f defined in eqn. 4 is not a state but an unknown inaccessible input and the conventional observer theory can be extended to estimate this input [15]. If the observer has a sufficiently fast dynamics as compared with the variation of the unknown disturbance, it can be assumed that the disturbance f is a constant during a short time interval as

$$\frac{df}{dt} = 0 \tag{19}$$

Under this assumption, f can be regarded as an additional state variable. Thus, the augmented state equation is given as

$$\dot{x}_a = A_a x_a + B_a u \tag{20a}$$

$$y_a = C_a x_a \tag{20b}$$

where

$$x_a = [\omega_r \ \ f]^T, \quad A_a = \begin{pmatrix} a_o & d_o \\ 0 & 0 \end{pmatrix},$$

$$B_a = \begin{pmatrix} b_o \\ 0 \end{pmatrix}, \quad C_a = [1 \ \ 0]$$

If the pair $\{A_a, C_a\}$ is completely observable, the unmeasurable state f can be reconstructed. Since these equations satisfy the observability condition, the full state observer to estimate the unknown disturbance can be given as follows [16]:

$$\dot{\hat{x}}_a = A_a \hat{x}_a + B_a u + L(y_a - C_a \hat{x}_a) \tag{21}$$

where L is the gain matrix of the observer defined as

$$L = \begin{pmatrix} l_1 \\ l_2 \end{pmatrix} \tag{22}$$

If the estimation error is chosen as

$$e = x_a - \hat{x}_a \tag{23}$$

the error dynamic equations of the observer are derived as

$$\dot{e} = (A_a - LC_a)e \tag{24}$$

The dynamic characteristics of the observer is determined by the eigenvalues of the matrix $(A_a - LC_a)$, which can be obtained by the characteristic equation given as

$$\det|pI - (A_a - LC_a)| = p^2 + 2\zeta\omega_n p + \omega_n^2 = 0 \tag{25}$$

where

$$\omega_n = \sqrt{d_o l_2}, \quad \zeta = -\frac{a_o - l_1}{2\omega_n}$$

From eqn. 25, the poles of the observer can be represented as

$$p_{1,2} = -\zeta\omega_n \pm \omega_n\sqrt{\zeta^2 - 1} \tag{26}$$

and the gain matrix L is easily obtained by the pole placement technique and using eqns. 25 and 26. To satisfy the assumption of eqn. 19 and obtain the good compensation performance, the dynamics of the observer should be chosen to be sufficiently fast as compared with the time variation of the disturbance. However, in practice, the selection of the observer pole is a compromise between the fast response and the insensitivity to the measurement noise. Fig. 8 shows the block diagram of the full state observer to estimate the unknown disturbance.

5 Simulations and experiments

5.1 Configuration of experimental system

The simulations and experiments are carried out for the BLDDM with the parameters as listed in Table 1.

Table 1: Specifications of BLDDM

Rated power	120W	Rated speed	123rev/min
Rated torque	11Nm	Rated voltage	120V
Poles	16	Stator resistance	9Ω
Stator	20 mH	Torque constant	3.038Nm/A
Moment of inertia	0.00398 Nm·s²	Damping coeff.	0.5 Nm·s

The configuration of the experimental system is shown in Fig. 9. The main processor of the experimental system is a floating-point DSP TMS320C30 with clock frequency of 33MHz. The BLDDM is driven by a three-phase voltage-fed PWM inverter using a MOSFET with a switching frequency of 10kHz. The brushless resolver is used to detect the position and speed of the BLDDM. The resolutions of the speed and position are calibrated as 0.1rev/min and 16 bit/rev, respectively. The phase currents are detected by the Hall-effect device and the detected analogue signals are converted to digital values by using the A/D converter with a 12-bit resolution. The sampling period of the proposed control scheme including the IVSC and load torque observer is set as 100μs.

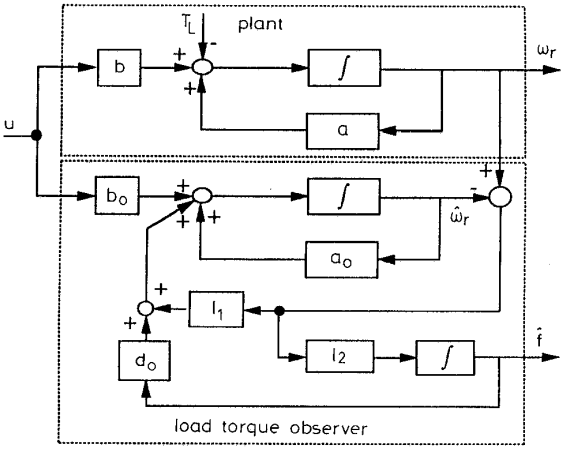

Fig.8 *Block diagram of proposed load torque observer*

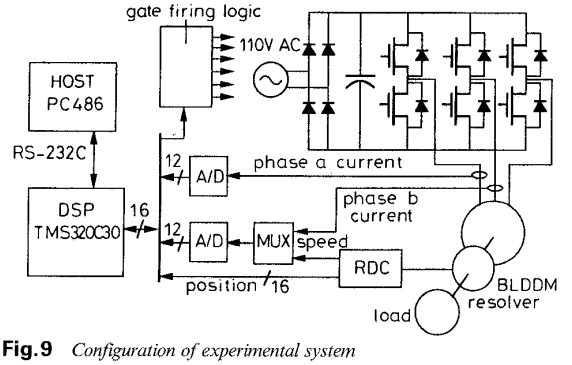

Fig.9 *Configuration of experimental system*

To examine the control performance of the proposed scheme under various load conditions, two types of load are considered as shown in Figs. 10–11. The dynamic behaviour of the control system can be tested under the inertia variation in the acceleration or deceleration region, and the steady-state performance can be examined by using the eccentric load which produces the load torque variation.

5.2 Current control of PWM inverter

In the BLDDM drive system, the current-control performance of the PWM inverter is very important because the speed control performance is directly influenced by the torque pulsation owing to the ripple of the stator current. The ramp-comparison controller

implemented using the software of the DSP is employed to control the stator current of the BLDDM. This controller has the advantage of limiting the maximum inverter switching frequency and producing well defined harmonics, but there exists unavoidable phase delay and steady-state error at high speed region [17]. However, since the BLDDM is generally operated at low speed, the effects of phase delay and steady-state error can be neglected. Therefore the use of the ramp-comparison controller is reasonable in the proposed control system and the modelling of the BLDDM in Section 2 can be regarded as a fair approximation.

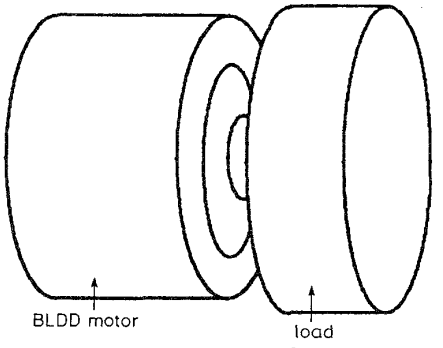

Fig. 10 *Inertia load used for simulations and experiments*

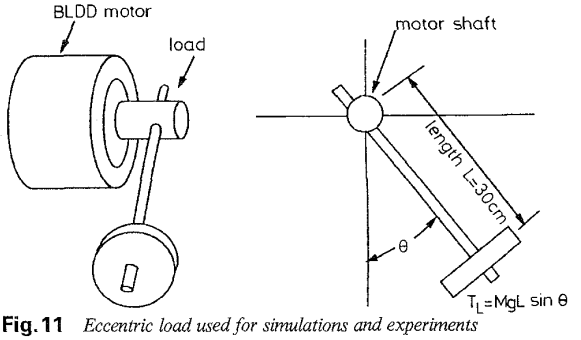

Fig. 11 *Eccentric load used for simulations and experiments*

5.3 Implementation of load torque observer and IVSC

The main control loop of the proposed scheme is composed of the IVSC and load torque observer. The sliding surface coefficient c_1 is chosen as 20. As mentioned in Section 3.1, the time constant of the closed-loop system can be determined as 50ms by this design. From eqn. 18 and under the assumptions of Δf_{max} = 0.6Nm and Δf_{min} = –0.6Nm, the gains of the switching control Δu are chosen as $\alpha_1 = 0.05$, $\beta_1 = -0.05$, $\alpha_2 = 0.2$, and $\beta_2 = -0.2$. The poles of the load torque observer are designed to have the Butterworth pole pattern and are chosen as $p_{1,2} = -200 \pm j200$ [16]. From eqn. 25, the gains of the load torque observer can be determined as $l_1 = 452$ and $l_2 = -96$. For the digital implementation of the load torque observer, the continuous-time representation of eqn. 21 is discretised by the simple backward difference method [18]. Since the sampling period of the proposed control scheme is chosen to be sufficiently faster than the time variation of the disturbance, this approximation can be acceptable in the simulations and experiments.

All of the proposed control algorithms including the current control of the PWM inverter, IVSC, and load torque observer are implemented by using the assembly language of DSP TMS320C30. These software development procedures are carried out by using TMS320C30 assembly language development tools including assembler, linker, and debugger [19, 20].

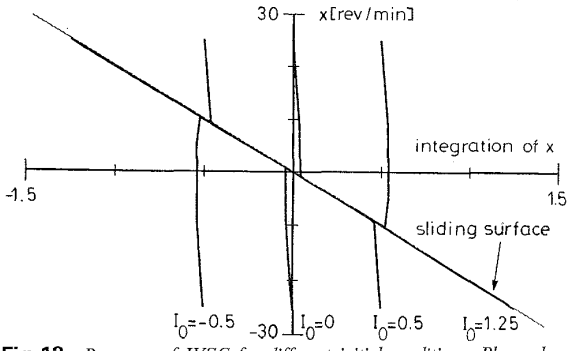

Fig. 12 *Response of IVSC for different initial conditions: Phase-plane trajectories*
$c_1 = 20$; $x_0 = -25$ rev/min; $\omega_{ref} = 25$ rev/min; $J_o = 0.00961$ Nms^2

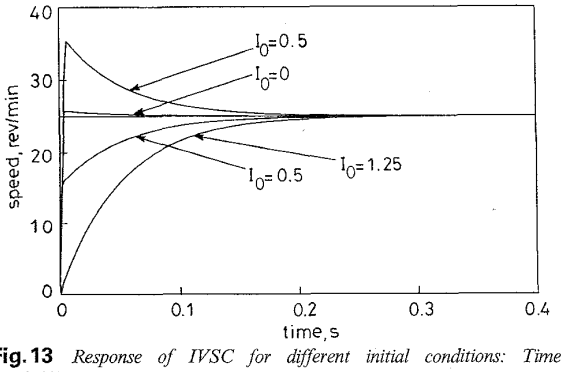

Fig. 13 *Response of IVSC for different initial conditions: Time responses*
$c_1 = 20$; $x_0 = -25$ rev/min; $\omega_{ref} = 25$ rev/min; $J_o = 0.00961$ Nms^2

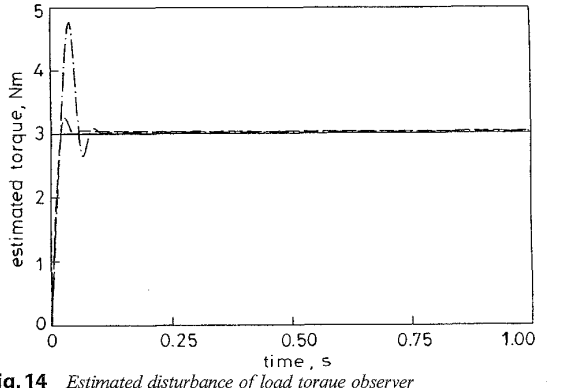

Fig. 14 *Estimated disturbance of load torque observer*
T_L = 3.0 Nm; J_o = 0.00961 Nms^2
——— real torque
– – – estimated torque ($J = J_o$)
—·—·— estimated torque ($J = 2J_o$)

5.4 Simulation results

To show the feasibility of the proposed control scheme, the computer simulations are carried out for the BLDDM drive system with various load conditions.

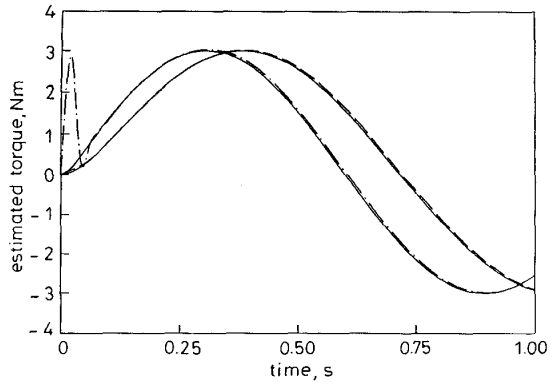

Fig. 15 *Estimated disturbance of load torque observer*
T_L = 3.0 sin (2 /$P\omega_r t$) Nm; J_o = 0.00961 Nms^2
——— real torque
– – – estimated torque ($J = J_o$)
—·—·— estimated torque ($J = 2J_o$)

Figs. 12 and 13 show the phase-plane trajectories and time responses of the IVSC for different initial conditions of the integrator. It is shown that the sliding mode is kept from the initial point when eqn. 11 is satisfied, i.e. $I_0 = 1.25$. Therefore the complete robustness can be ensured by properly choosing the initial condition of the integrator in the IVSC.

The estimating performance of the load torque observer is shown in Figs. 14 and 15. These Figures show that the large overshoot occurs when $J = 2J_o$. This means that the load torque observer estimates the effective load torque represented as

$$T_{eff} = T_L + \Delta J \left(\frac{2}{P}\right) \frac{d\omega_r}{dt} \tag{27}$$

rather than the load torque T_L. Therefore the effect of the inertia variation can also be compensated by using the load torque observer. The second term in the right-hand side of eqn. 27, that is the disturbing torque caused by the inertia variation, is dominant at high acceleration or deceleration. However, since the disturbance is assumed as constant in eqn. 19, the estimation error of the load torque observer is increased in this region and thus the speed control performance may also be degraded. However, in the proposed control scheme, since the effect caused by the disturbance estimation error can be rejected by the IVSC, the speed control performance is not greatly influenced by this effect.

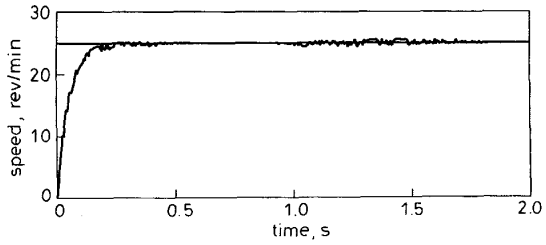

Fig. 16 *Speed responses of IVSC without disturbance compensation*
T_L = 3.0 sin (2 /$P\omega_r t$) Nm; J_o = 0.00961 Nms^2

Figs. 16–19 illustrate the effectiveness of the disturbance compensation using the load torque observer. Figs. 16 and 17 show the speed responses and control inputs of the IVSC without the disturbance compensation, and Figs. 18 and 19 show with the disturbance compensation. The input chattering is remarkably reduced by the disturbance compensation using the load torque observer.

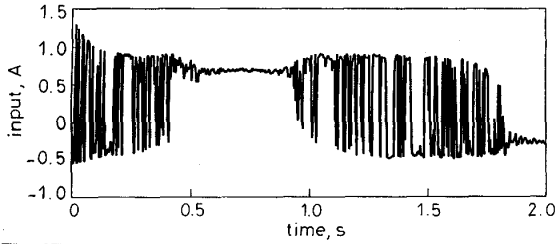

Fig. 17 *Control inputs of IVSC without disturbance compensation*
T_L = 3.0 sin (2 /$P\omega_r t$) Nm; J_o = 0.00961 Nms^2

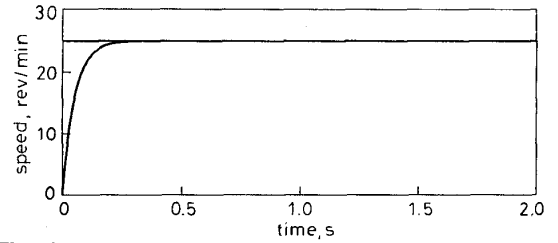

Fig. 18 *Speed responses of IVSC with disturbance compensation*
T_L = 3.0 sin (2 /$P\omega_r t$) Nm; J_o = 0.00961 Nms^2

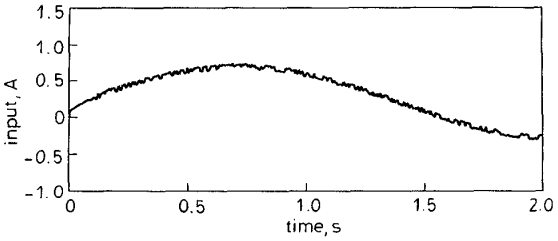

Fig. 19 *Control inputs of IVSC with disturbance compensation*
T_L = 3.0 sin (2 /$P\omega_r t$) Nm; J_o = 0.00961 Nms^2

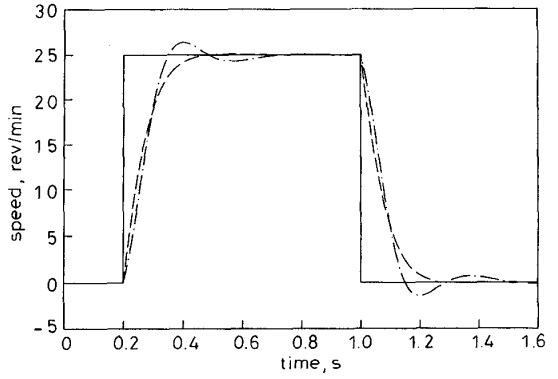

Fig. 20 *Transient responses of PI with torque observer under inertia variation*
— — — $J = J_o$
—·—·— $J = 2J_o$
J_o = 0.00961 Nms^2

The speed control performance of the proposed scheme is compared with that of the PI control with the load torque observer. Figs. 20 and 21 show the dynamic performance of both schemes under the inertia variations. The PI controller is well tuned in the nominal condition, i.e. $J = J_o$. When $J = 2J_o$, it is observed that the overshoot becomes about 10% of the

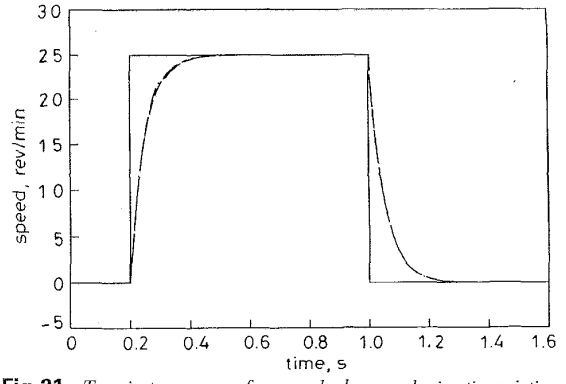

Fig. 21 *Transient responses of proposed scheme under inertia variation*
— — — $J = J_o$
—·—·— $J = 2J_o$
$J_o = 0.00961$ Nms^2

reference in the PI control. This result is caused by the estimation errors of the torque observer because the time variations of effective load torque is very fast in this condition. To reduce the undesirable overshoot it is required that the torque observer has the fast dynamics which can be achieved by choosing the large observer gain. However, it is difficult to realise in practice because of measurement noise and the numerical errors of the digital processor. Therefore the effects of the estimation error should be rejected by the feedback controller. Since this effect is fully rejected by the switching control of the IVSC in the proposed scheme, the robust control performance can be obtained under the inertia variations.

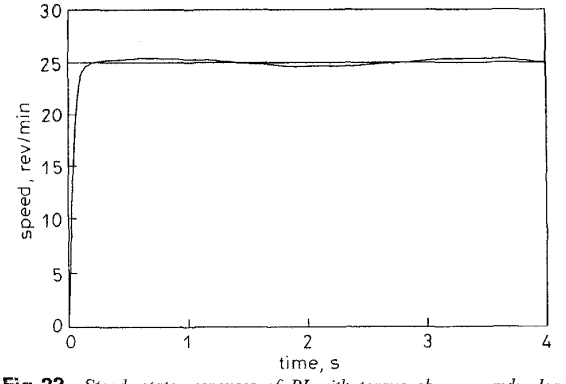

Fig. 22 *Steady-state responses of PI with torque observer under load torque variation*
$T_L = 3.0 \sin (2/P\omega_r t)$ Nm; $J_o = 0.0491$ Nms^2

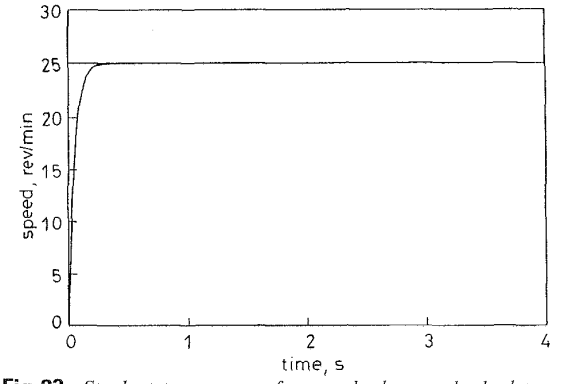

Fig. 23 *Steady-state responses of proposed scheme under load torque variation*
$T_L = 3.0 \sin (2/P\omega_r t)$ Nm; $J_o = 0.0491$ Nms^2

Figs. 22 and 23 show the steady-state performance of both schemes when the external load is sinusoidally varied. It can be also observed that the proposed scheme has the robustness against the load torque variation. In the PI controller, the ability of the disturbance rejection can be expanded by increasing the gain of the integrator, but the high gain of the integrator causes the undesirable effects such as the high overshoot and long settling time due to the saturation of the integrator, called 'integral wind-up'.

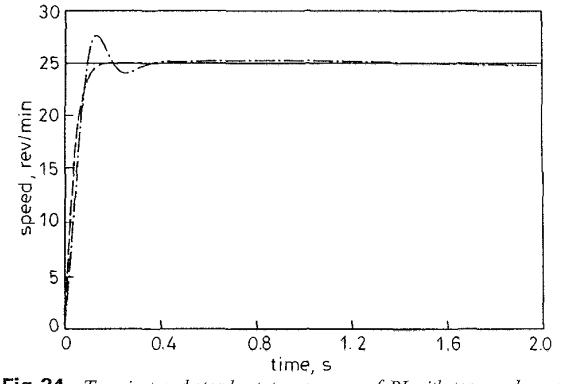

Fig. 24 *Transient and steady-state responses of PI with torque observer under inertia and load torque variations*
——— $J = J_o$, $T_L = 0$
—·—·— $J = 2J_o$, $T_L = 3.0 \sin (2\ \omega t/P)$
$J_o = 0.00961$ Nms^2

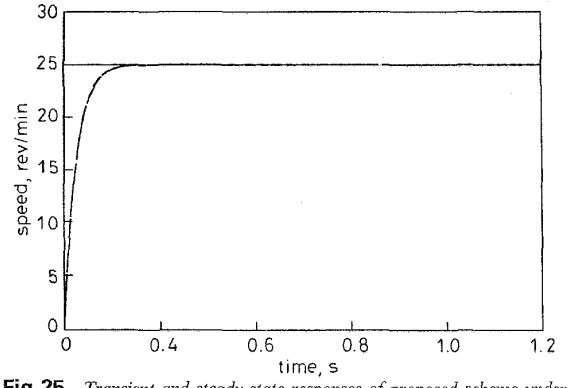

Fig. 25 *Transient and steady-state responses of proposed scheme under inertia and load torque variations*
——— $J = J_o$, $T_L = 0$
—·—·— $J = 2J_o$, $T_L = 3.0 \sin (2\ \omega t/P)$
$J_o = 0.00961$ Nms^2

Figs. 24 and 25 show the transient and steady state performance of both schemes when the combinational load of Figs. 10 and 11 is applied. As predicted from previous results, it is well demonstrated that the proposed control scheme provides a robust control performance in both transient and steady states.

5.5 Experimental results

In this Section the experimental results are discussed for the two types of load condition as shown in Figs. 10 and 11. The PI control with the torque observer scheme is tuned to have the critically damped response and the settling time is chosen as 200ms. The same design parameters given in Section 5.3 are used in the proposed control scheme.

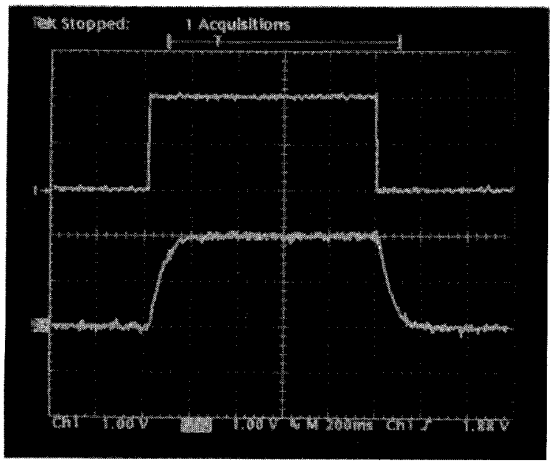

Fig.26 *Transient responses of PI with torque observer ($J = J_o$) under inertia variation*
Upper traces: Speed reference, lower traces: Real speed, 12.5 rev/min/div. Horizontal scale: 200 ms/div., J_o = 0.00961 Nms^2

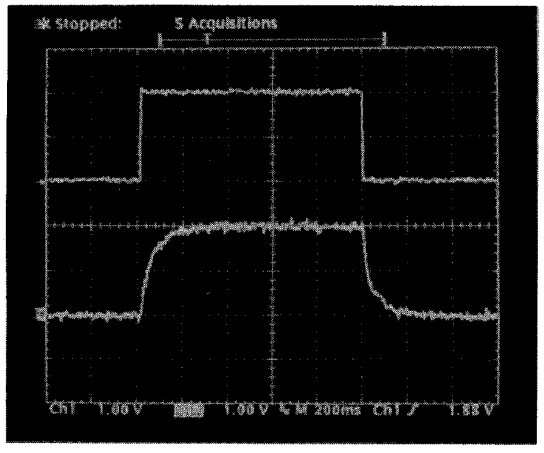

Fig.27 *Transient responses of proposed scheme ($J = J_o$) under inertia variation*
Upper traces: Speed reference, lower traces: Real speed, 12.5 rev/min/div. Horizontal scale: 200 ms/div., J_o = 0.00961 Nms^2

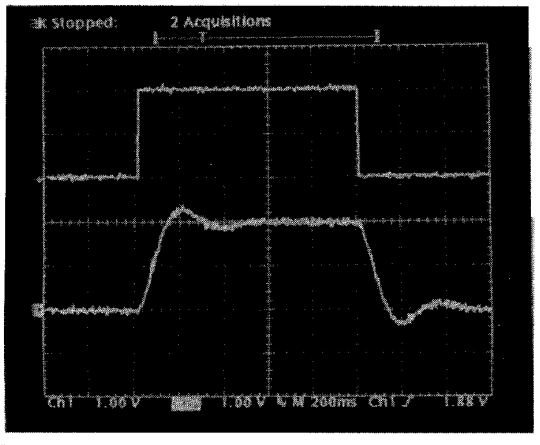

Fig.28 *Transient responses of PI with torque observer ($J = 2J_o$) under inertia variation*
Upper traces: Speed reference, lower traces: Real speed, 12.5 rev/min/div. Horizontal scale: 200 ms/div., J_o = 0.00961 Nms^2

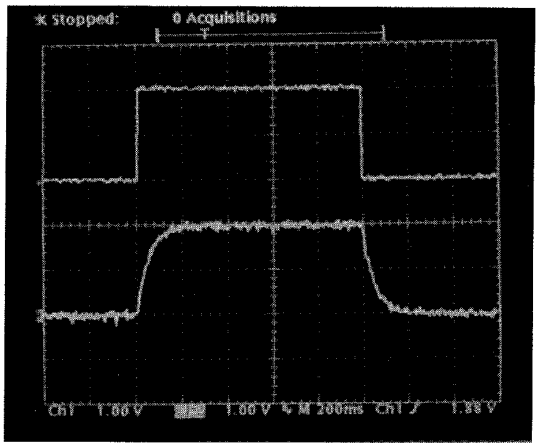

Fig.29 *Transient responses of proposed scheme ($J = 2J_o$) under inertia variation*
Upper traces: Speed reference, lower traces: Real speed, 12.5 rev/min/div. Horizontal scale: 200 ms/div., J_o = 0.00961 Nms^2

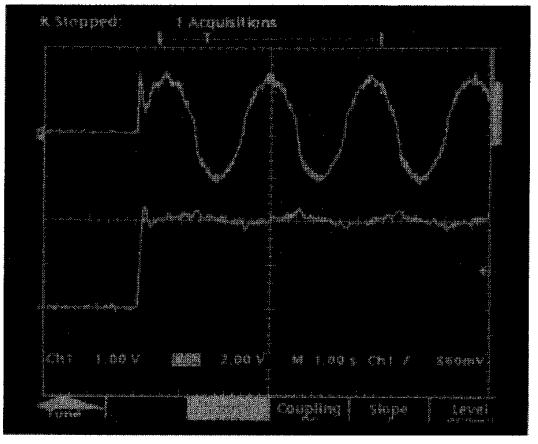

Fig.30 *Steady-state responses of PI with torque observer under load torque variation*
Upper trace: Estimated torque 3 Nm/div., lower traces: Real speed 12.5 rev/min/div. Horizontal scale: 1 s/div., $T_L = Mgl \sin(2/P\omega_r t)$, M = 1.0 kg, l = 30 cm, J_o = 0.0491 Nms^2

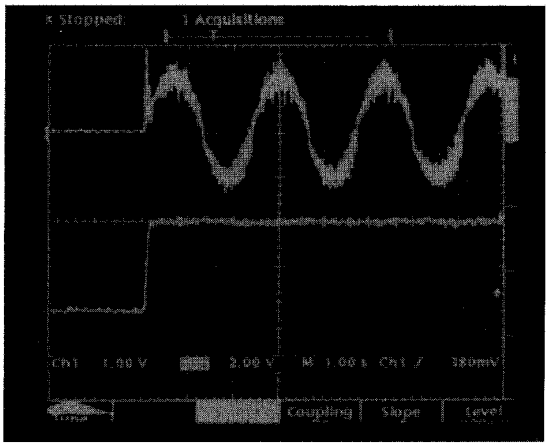

Fig.31 *Steady-state responses of proposed scheme under load torque variation*
Upper trace: Estimated torque 3 Nm/div., lower trace: Real speed 12.5 rev/min/div. Horizontal scale: 1 s/div., $T_L = Mgl \sin(2/P\omega_r t)$, M = 1.0 kg, l = 30 cm, J_o = 0.0491 Nms^2

The dynamic responses of both schemes under the inertia variation are shown in Figs. 26–29. Both controllers provide a good dynamic response corresponding the design specifications when $J = J_o$. However, when the inertia is doubled in the PI with the torque observer scheme, the overshoot and settling time are increased as 10% and 400ms, respectively. However, the proposed scheme provides the same responses in both cases.

The steady-state responses of both schemes are shown in Figs. 30 and 31 when the load described in Fig. 11 is applied. In Fig. 30, the speed fluctuation is shown because of the estimation errors in the torque observer. However, as shown in Fig. 31, a good speed regulation is achieved in the proposed control scheme.

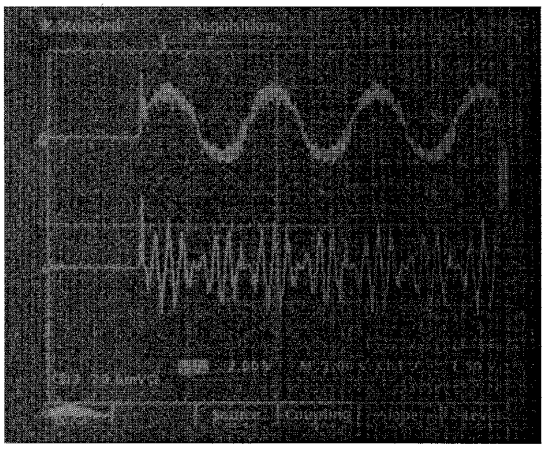

Fig. 32 *Control input and phase current of proposed control scheme*
Upper trace: Control input 1 A/div, lower trace: Phase current 1 A/div. Horizontal scale: 1 s/div., $T_L = Mgl \sin(2/P\omega_r t)$, $M = 1.0$ kg, $l = 30$ cm, $J_o = 0.0491$ Nms^2

Fig. 32 shows the control input and phase current of the proposed scheme. If the disturbance compensation loop is not employed, the large switching control of about 1.0A is required for the rejection of the torque variation effects. However, in the proposed control scheme, it is shown that the level of the switching control is greatly reduced to about 0.2A.

6 Conclusions

This paper described a robust speed control technique for the BLDDM using a VSC approach. The practical limitations of the conventional VSC approach for the speed control of BLDDM were investigated and the IVSC with a load torque observer scheme proposed as an effective way of overcoming the problems in the conventional VSC. The design methods of the proposed IVSC and load torque observer have been given and the designed control method applied to the DSP-based BLDDM drive system. To show the effectiveness of the proposed control scheme, the comparative simulations and experiments were carried out under the various load conditions. The distinctive results of this study are summarised as follows.

Unlike the conventional approaches, the IVSC is suitable for the system having the first-order dynamics. Thus, the IVSC is directly applicable for the speed control system of the BLDDM without any informations on the acceleration. The initial condition of the integrator to satisfy the perfect robustness is derived and it is shown that the sliding mode is ensured from the beginning of the response without the reaching problem. The chattering is successfully reduced by the disturbance compensation technique using the load torque observer. As compared with PI control with the load torque observer scheme, the proposed IVSC scheme combined with the load torque observer provides a good control performance in both transient and steady-states. These results well verify that the proposed control scheme has the robustness against the unknown disturbance. It is therefore expected that the proposed control scheme can be applied to the high performance applications of BLDDMs such as the high precision control of machine tools and industrial robots. These applications are being considered as one of our further research subjects.

7 References

1 FURUTA, K., KOSUGE, K., and KOBAYASHI, K.: 'Self-tuning, sliding mode, and adaptive control for direct drive motor'. IEEE IECON '88 conference record, 1988, pp. 459–165
2 FURUTA, K., KOSUGE, K,. and KOBAYASHI, K.: 'VSS-type self-tuning control of direct drive motor'. IEEE IECON '89 conference record, 1989, pp. 281–286
3 FURUTA, K., and KOBAYASHI, S.: 'Bang-bang position control of direct drive motor'. IEEE IECON '90 conference record, 1990, pp. 148–153
4 MATSUI, N., MAKINO, T., and SATOH, H.: 'Auto compensation of torque ripple of direct drive motor by torque observer', *IEEE Trans.*, 1993, **IA–29**, (1), pp. 187–194
5 LEE, J.H., KO, J.S., CHUNG, S.K., LEE, J.J., and YOUN, M.J.: 'Design of continuous sliding mode controller for BLDDM with prescribed tracking performance'. IEEE PESC '92 conference record, 1992, pp. 770–775
6 KAWAMURA, A., MIURA, K., and ISHIZAWA, T.: 'Trajectory control of two axis scara robot by sliding mode control with observer'. IEEE IECON '88 conference record, 1988, pp. 640–645
7 DOTE, Y., TAKABE, M., and ITO, T.: 'Variable structure control with sliding mode for dc drive speed regulation'. IEEE PESC '82 conference record, 1982, pp. 123–127
8 NANDAM, P.K., and SEN, P.C.: 'Sliding mode speed control of a self-controlled synchronous motor based on state estimation (observer) and digital differentiation'. Proceedings of IPEC '90, 1990, pp. 291–295
9 HARASHIMA, F., HASHIMOTO, H., and KONDO, S.: 'MOSFET converter-fed position servo system with sliding mode control', *IEEE Trans.*, 1985, **IE–32**, (3), pp. 238–244
10 HASHIMOTO, H., MARUYAMA, K., and HARASHIMA, F.: 'A microprocessor-based robot manipulator control with sliding mode', *IEEE Trans.*, 1987, **IE–34**, (1), pp. 11–18
11 HASHIMOTO, H., YAMAMOTO, H., YANAGISAWA, S., and HARASIMA, F.: 'Brushless servo motor control using variable structure approach', *IEEE Trans.*, 1988, **IE–34**, (1), pp. 160–170
12 CHERN, T.L., and WU, Y.C.: 'Design of brushless DC position servo systems using integral variable structure approach', *IEE Proc. B*, 1993, **140**, (1), pp. 27–34
13 PARK, G.T., CHOI, J.K., and KIM, D.S.: 'The design of variable structure controller for the systems having the first order dynamics', *J. Korean Inst. Electr. Eng.*, 1992, **41**, (4), pp. 392–399
14 KRAUSE, P.C.: 'Analysis of electric machinery' (McGraw–Hill, 1986)
15 MEDITCH, J.S., and HOSTETTER, G.H.: 'Observers for systems with unknown and inaccessible inputs', *Int. J. Control*, 1974, **19**, (3), pp. 473–480
16 FRANKLIN, G.F., POWELL, J.D., and EMAMI-NAEINI, A.: 'Feedback control of dynamic systems' (Addison–Wesley, 1986)
17 BROD, D.M., and NOVOTNY, D.W.: 'Current control of VSI-PWM inverters', *IEEE Trans.*, 1985, **IA–21**, (2), pp. 562–570
18 OGATA, K.: 'Discrete-time control system' (Prentice–Hall, 1987)
19 TMS320C3x User's Guide. Texas Instrument, 1990
20 TMS320C30 Assembly Language Tools User's Guide. Texas Instrument, 1990